Tetrahedron 67 (2011) 7400–7405

Contents lists available at ScienceDirect

Tetrahedron

journal homepage: www.elsevier.com/locate/tet

Role of edge-to-face interaction between aromatic rings in clathrate formation of 1-benzoyl-2-hydroxyindoline derivatives with benzene. X-ray crystal and PM6 analyses of the interaction

Masashi Eto *, Koki Yamaguchi, Itaru Shinohara, Fumikazu Ito, Yasuyuki Yoshitake, Kazunobu Harano

Faculty of Pharmaceutical Sciences, Sojo University, 4-22-1 Ikeda, Kumamoto 860-0082, Japan

ARTICLE INFO

Article history:
Received 7 June 2011
Received in revised form 6 July 2011
Accepted 9 July 2011
Available online 3 August 2011

Keywords:
Edge-to-face interaction
CH/O interaction
1-Benzoyl-2-hydroxyindoline
PM6 calculation

ABSTRACT

(4-Nitrophenyl- and 4-chlorophenyl)(2-hydroxy-3,3-dimethylindolin-1-yl)methanone (**4a**,**b**) serve as clathrate hosts for benzene guests. X-ray crystal analyses of the inclusion compounds of **4a** and **4b** with benzene indicate that the 'edge-to-face interaction' plays an important role in the formation of the inclusion complexes with benzene as well as in the host–host interactions. PM6 molecular orbital calculations were found to reproduce the characteristic structural features of both intra- and intermolecular edge-to-face interactions.

1. Introduction

The CH/π interaction can be regarded as a weak hydrogen bond, which occurs between a soft acid and a soft base. Nishio et al.[1,2] indicated that the CH/π interaction is not only a conventional *van der* Waals force but also has hydrogen-bond-like properties. High-level *ab initio* molecular orbital (MO) calculations support this concept. The enthalpy of a single-unit CH/π interaction is small (around 1 kcal/mol). However, CH/π interactions have been shown to play significant roles in various fields of chemistry, e.g., in determining the conformation of molecules, crystal packing and in the assembly of molecular units into an organized supramolecular structure. It has also been suggested the CH/π interaction plays an important role in the structure of proteins and DNA.[3]

During the course of the studies[4] of the isolable atropisomers caused by restricted rotation around the Csp^3–Csp^2 bond of [2-(2-hydroxynaphthalen-1-yl)-3,3-dimethyl-2,3-dihydroindol-1-yl](4-nitrophenyl)methanone (**5a** and **6a**), we recognized the formation of a crystalline inclusion compound of **4a** (Scheme 1) with benzene. The inclusion behavior of **4** is discussed in this study along with newly obtained X-ray diffraction data, which are used to clarify the overall character of the hydroxylic hosts.

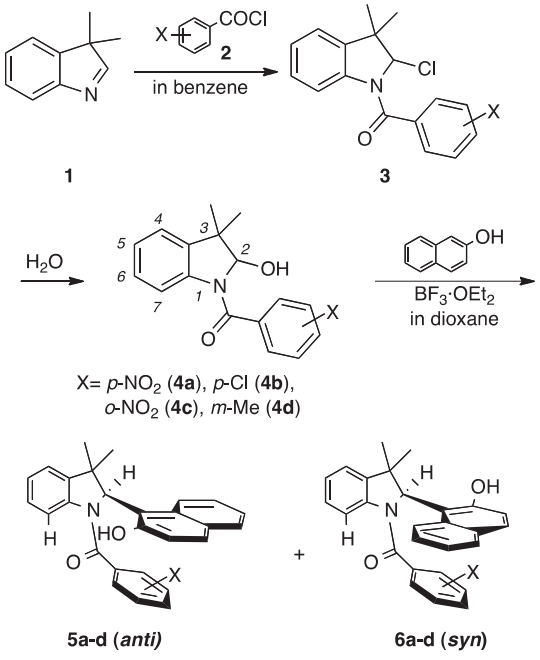

Scheme 1.

* Corresponding author. E-mail address: meto@ph.sojo-u.ac.jp (M. Eto).

0040-4020/$ – see front matter © 2011 Elsevier Ltd. All rights reserved.
doi:10.1016/j.tet.2011.07.021

2. Results

2.1. Inclusion properties

The host compounds (**4a**–**d**) were synthesized by treatment of the corresponding 2-chloro derivatives (**3a**–**d**) with water.[4c] A variety of solvents (benzene, acetone, chloroform, ethanol, and toluene) were used to explore the inclusion properties of **4a**–**d**. The inclusion compounds were obtained by slow evaporation of a solution of the host compounds in the respective guest solvents at ambient temperature. Of several substituted benzoyl derivatives, the 4-nitro (**4a**) and 4-chlorobenzoyl (**4b**) derivatives formed the 2:1 inclusion complexes with benzene. The host: guest stoichiometric ratio was confirmed by thermogravimetric (TG) analysis. The total weight loss was observed to be 10.4% for **4a**·benzene and 10.0% for **4b**·benzene, in close agreement with the expected losses of 11.1% and 11.5%, respectively, for a 2:1 host/guest ratio (see the Supplementary data, Figs. S1 and S2).

2.2. X-ray analysis

*2.2.1. **4a**·Benzene and **4b**·benzene complexes.* The ORTEP[5] representations of **4a**·benzene and **4b**·benzene are depicted in Fig. 1, in which each complex has one-half of a benzene molecule in the asymmetric unit, with the other half generated by a crystallographic inversion center.

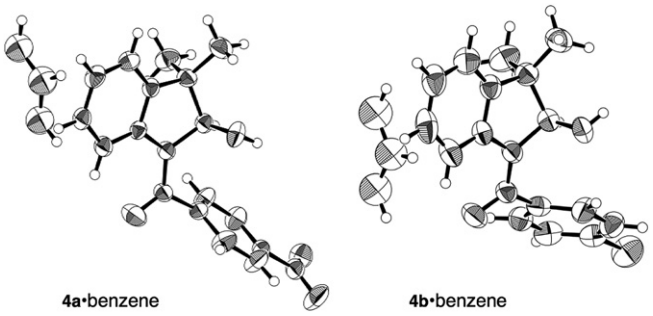

Fig. 1. ORTEP drawings of **4a**·benzene and **4b**·benzene inclusion complexes.

In both structures, the amide carbonyl oxygen is oriented toward the C7–H of the indoline moiety and the aryl ring is not coplanar with the >NCO– plane. The interatomic distances between the amide carbonyl oxygen and C7–H are 2.320 (4) Å (**4a**) and 2.401 (3) Å (**4b**), indicating of the presence of CH/O-type hydrogen bonding.[6]

In the crystal structure of **4a**·benzene, inclusion of the guest (benzene) molecule is facilitated by edge-to-face (or T-shape) aromatic CH/π interactions between the four indoline benzene rings, suggesting the presence of potential CH/π interactions in which the benzene rings act as both hydrogen-bond donor and acceptor (Fig. 2 and S4). The H_a proton of the host benzene molecule is located at a close-contact perpendicular distance of 2.796 Å above the face of the indoline ring. Additionally, the edge-to-face distance between the C5–H of the indoline ring and the plane of the guest π-system was 3.167 Å.

The host molecules are linked by π–π and edge-to-face interactions, depicted in Fig. 3a and b. There are two types of π–π interaction between the 4-nitrobenzoyl rings. The π–π interaction stacking distance between the 4-nitrobenzoyl rings is considerably shorter than the typical values (<3.6 Å), which is the result of an additional coulombic interaction force between the benzoyl carbonyl oxygen and the nitrogen atom of the nitro group [O···N, 2.899 (5) Å]. Another mode of π–π interaction stacking is found

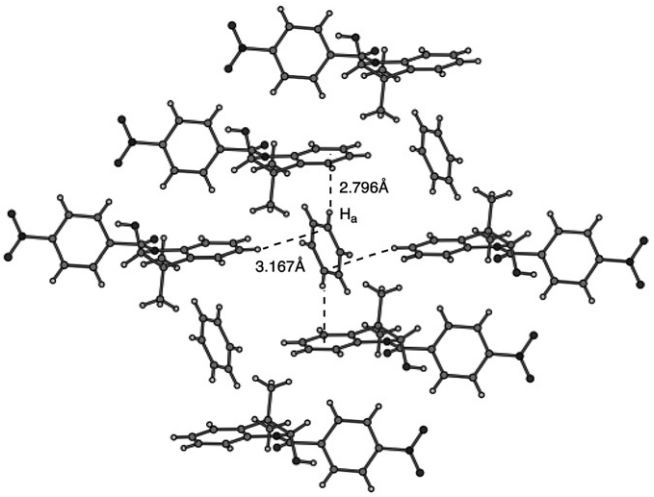

Fig. 2. Edge-to-face interactions between the host (**4a**) and guest (benzene) molecules.

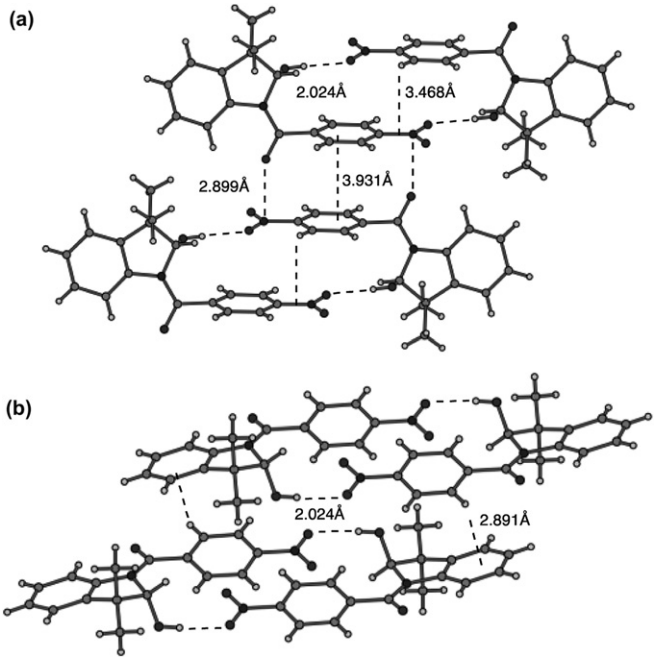

Fig. 3. (a) π–π Interactions between the host molecules (**4a**) and (b) edge-to-face interactions between the host molecules (**4a**).

between the 4-nitrobenzoyl rings; this is facilitated by the hydrogen bond between the nitro group and the 2-hydroxy group of the indoline moiety [O···O, 2.838 (5) Å; O–H···O, 2.024 (4) Å]. Edge-to-face interactions between the host molecules were observed, in which the distance between the *ortho* proton of the benzoyl group and the neighboring indoline ring is 2.891 Å (Fig. 3b).

The crystal structure of the inclusion complex **4b**·benzene is depicted in Fig. 4 (see Fig. S5). The marked difference in inclusion behavior between **4a** and **4b** indicates recognition of hydrogen on the guest by the host molecules. The benzene hydrogens interact with the oxygen atoms of the hydroxy and benzoyl groups of the host molecules *via* CH/O-type hydrogen bonds.[6] In contrast, the CH/π interaction between the π plane of the benzene (guest) and the host molecule (**4b**) is similar to that observed in **4a**, in which the distance between the C4–H and the plane of the guest benzene is 2.916 Å. In the inclusion complex, the host molecules are firmly bounds together by C=O/H–O hydrogen bonds [O–(H)···O, 2.665 (4) Å, O–H···O, 2.016 (3) Å].

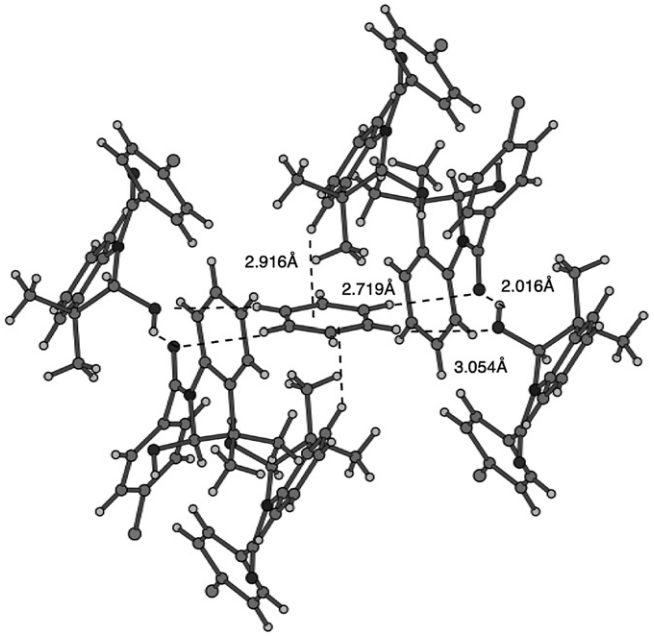

Fig. 4. Edge-to-face and CH/O interactions in clathrate of 4b·benzene.

*2.2.2. Guest-free host (**4c**).* The crystal structure of the free host **4c** is depicted in Fig. 5. The host molecules are linked by intermolecular hydrogen bonds between the amide carbonyl oxygen and the 2-hydroxy group of the neighboring molecule [O–(H)···O, 2.764 (4) Å, O–H···O, 1.953 (3) Å]. In contrast to the case for **4a**, the 2-nitro group does not form a hydrogen bond with the 2-hydroxy group. The benzoyl ring interacts with the adjacent indoline benzene ring in an overlapping face-to-face manner, thus stabilizing the host network. The closest interatomic distance between the carbon atoms is 3.52 (1) Å.

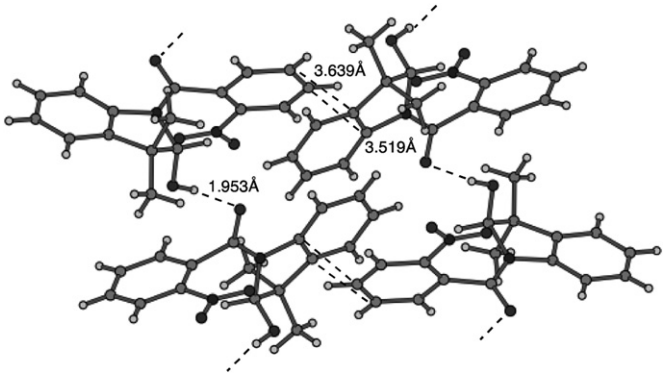

Fig. 5. Guest-free host–host interactions of **4c**.

3. Discussion

The hydroxylic host compound **4a** enclathrated guest benzene molecules with a 2:1 host/guest stoichiometric ratio. The host–host framework is assembled by tight hydrogen bonds between the 4-nitro group of the benzoyl ring and the 2-hydroxy group of the indoline ring. In addition to this, the dimeric host molecules are linked intermolecularly in edge-to-face and face-to-face manner by interaction between the aryl groups (Fig. 3). The benzene guest is located inside the space surrounded by four aryl groups stabilized by CH/π interactions.

Semi-empirical MO calculations were performed in order to assess the geometric features involving weak intermolecular interactions such as the edge-to-face interaction forces between aromatic π rings. The objective was to determine whether the guest benzene is hold by edge-to-face interactions during optimization, in which a partial structure (six hosts and three guests) of the crystal packing diagram of **4a** is used, as shown in Fig. 6.

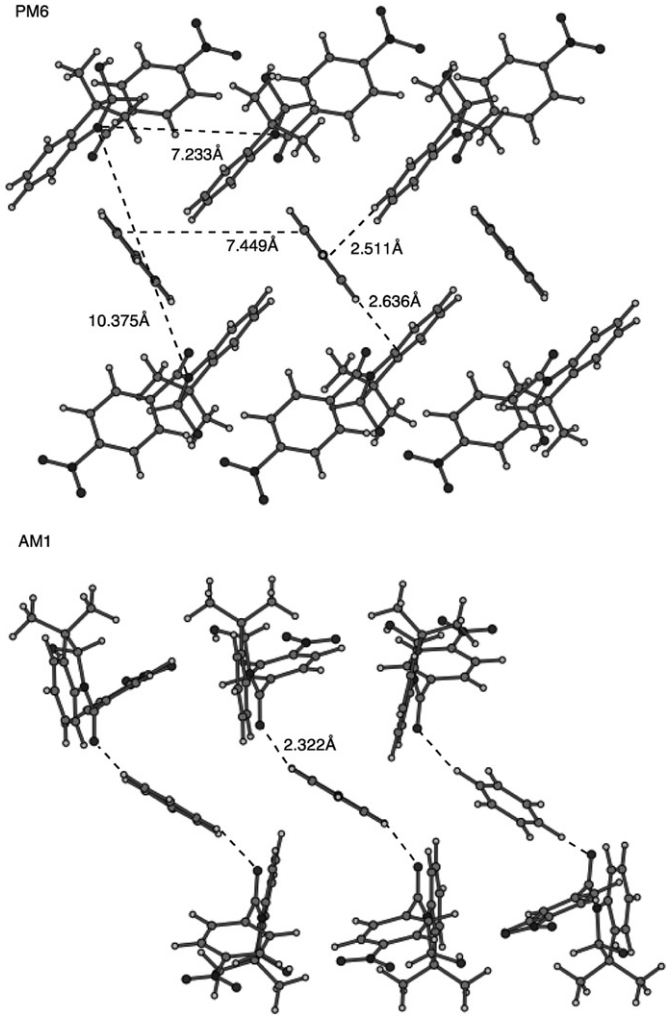

Fig. 6. PM6- and AM1-calculated partial packing structure of 4a·benzene complex looking through the central benzene molecule.

The geometry of the complex was fully optimized by AM1,[7] PM3,[8] and PM6[9] methods without imposing any symmetrical restrictions. The X-ray structure and PM6-calculated interatomic distances, intermolecular edge-to-face interaction distances and interplane distances are summarized in Table 1.

Table 1
Comparison of the important distances between the crystal structure (**4a**·benzene) and the computed structure

	Distance (Å)	
	X-ray	PM6[a]
Host/host		
N (amide)···N (amide) [cross]	10.978 (5)	10.375
N (amide)···N (amide)	7.189 (4)	7.233
Guest/guest		
C···C	7.19 (1)	7.449
Host/guest		
Guest-H···host indoline benzene ring	2.796	2.636
Guest plane···C6–H of host indoline ring	3.167	2.511

[a] Average. For atomic coordinates see Table S7.

The results show that the newly parameterized PM6 calculation approximately reproduced the spatial orientation of the guest molecule, whereas the AM1 and PM3 methods did not show satisfactory results (Fig. 6).[10]

In the AM1-optimized geometry, there was no evidence of the characteristic structural features of the edge-to-face interaction; instead, weak CH/O-type interactions between the carbonyl oxygen atom of the host and the hydrogen atom of benzene (guest) operate in place of edge-to-face interactions. The PM6 stabilization energy of benzene arising from its inclusion by four edge-to-face interactions (Fig. 2) is estimated to be 3.90 kcal/mol.[11] This result seems to be reliable because high-level *ab initio* MO calculations[12] suggest that the enthalpy of a single-unit CH/π interaction is around 1 kcal/mol. As shown in Figs. 2 and 6, the edge-to-face structural features were approximately reproduced by PM6 calculation. Inspection of the intermolecular distances indicates that the distance between the benzene-ring plane of the guest molecule and the hydrogen atom of the phenyl group of the neighboring host molecule is significantly short. This may be the result of a movement of the edge-to-face interaction position on the guest plane from the *peri* position of benzene (X-ray structure) to the central position of the guest in the PM6-calculated geometry.

The host **4c** did not enclathrate any guest molecules. This lack of the inclusion ability toward benzene can be attributed to the host–host network mode. By replacing 4-nitrobenzoyl with a 2-nitrobenzoyl group, the host becomes tightly linked by intermolecular hydrogen bonding between the 2-hydroxy group and the amide carbonyl oxygen of the neighboring molecules. It is interesting to note that the nitro group of **4c** does not form hydrogen bonds despite its strong hydrogen-bond acceptor ability. In addition, aryl–aryl interactions between the indoline rings further stabilize the host network.

The host **4b** enclathrated benzene with a 2:1 host/guest ratio. However, the inclusion pattern of the guest is different from that of **4a**. Comparison of the inclusion behavior of **4a** with that of **4b** suggests that the replacement of the 4-nitro group by the chloro group causes a change in the host–host network, resulting in the recognition mode toward benzene.

These findings in **4a**–**c** suggest that the hydrogen-bond network between the host molecules plays an important role in complex formation with guests.

On the basis of these findings, the inclusion behavior of **5d** was reinvestigated. During a synthetic study of the atropisomers (**5**), it was found that **5d** (*anti*)[4g] formed a crystalline inclusion complex[13] with the recrystallization solvent (acetone). A computer-generated drawing of the crystal structure of inclusion complex **5d**·acetone is depicted in Fig. 7.

In the crystal packing, the host molecules form a dimeric unit linked by hydrogen bonds between the amide carbonyl and the naphthyl OH group [C=O···(H)–O, 2.666 (7) Å; O···H–O, 1.861 (5) Å], resulting in a 16-membered cyclic hydrogen-bonded structure. The edge-to-face interaction is found between the aromatic protons of the benzoyl group and the indoline moiety. The closest distances between the carbon atoms are 3.87 (1) and 3.90 (1) Å. In addition, the dimeric host molecules are considered to be intermolecularly linked by a CH/N interaction between the 3-methyl group of the benzoyl ring and the amide group conjugated with the phenyl ring of the indoline moiety.[14] The methyl group is located almost perpendicularly to the amide plane. The interatomic distance between the methyl carbon atom and the nitrogen atom is 3.82 (1) Å. In the previous paper, we reported that the presence of the intramolecular ArOH/N interactions of **5** (*anti* isomer) affects the stabilization of the rotamers based on the DFT calculations and the equilibrium constants including the solvent and the substituents effects,[4j] in which the amide nitrogen atom acts as a hydrogen-bond acceptor.[15] Inspection of the PM6 calculation data of

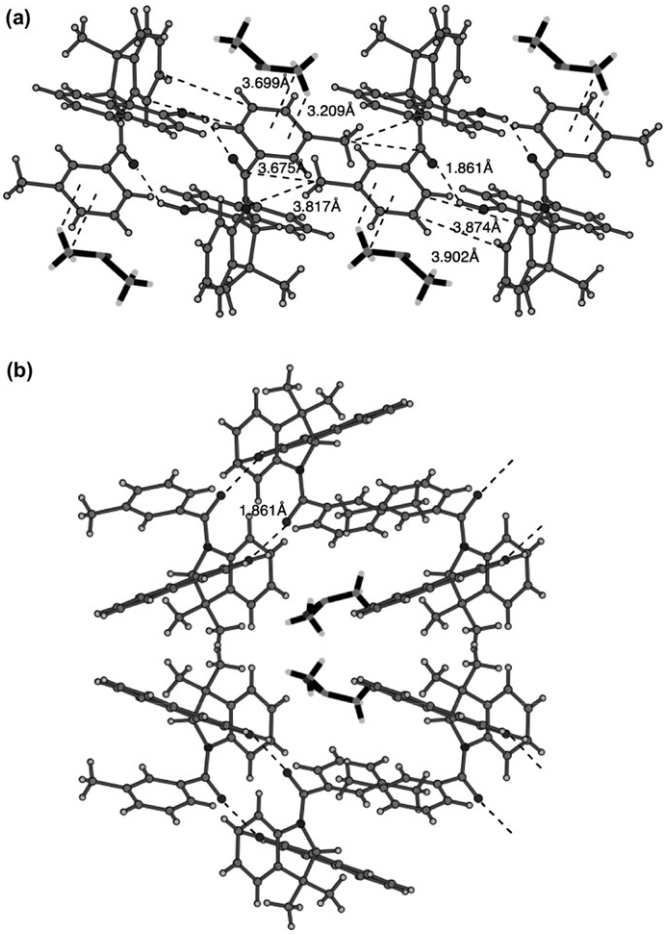

Fig. 7. Crystal structure of **5d**·acetone complex.

5d indicate that the amide nitrogen has a large negative charge (−0.418) and HOMO coefficient, suggesting that the attractive coulombic interaction and the favorable orbital interaction between the nitrogen atom and CH group can be expected (Fig. 8).

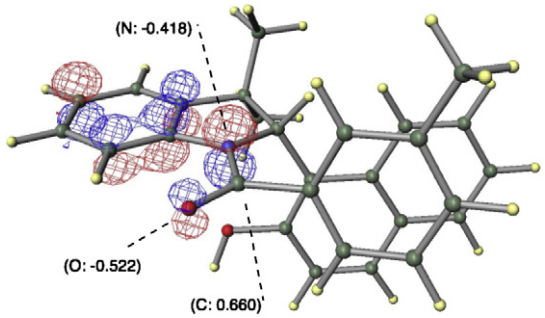

Fig. 8. HOMO of **5d** (net charges are shown in parentheses).

The guest structure of the complex is disordered in the crystal. The guest acetones are aligned almost parallel along the *c*-axis; however, only an approximate structure can be obtained by the calculation of differential Fourier synthesis. Inspection of the packing structure suggests that the acetone molecule assumes several possible orientations related by rotation around the carbonyl carbon atom. One of the possible models is shown in Fig. 7, in which the oxygen was assigned based on the highest Fourier peak.

In this model, along the cavity created by the host dimers, the methyl hydrogen of the guest seems to be linked with the carbonyl oxygen of neighboring guests by weak CH/O interactions [C=

O···(H)–C, 3.67 (2) Å]. A weak CH/π interaction is expected between the benzoyl ring and one of the methyl group of the acetone, in which the distance between the methyl hydrogen atom and the least-squares plane of the phenyl ring is 3.70 Å [C–(H)···plane, 3.21 Å].

To assess the guest orientation, the PM6 calculation was performed for the partial structures extracted from the inclusion complex (18 hosts and six guests; Fig. 9), in which only the guest molecules were optimized.

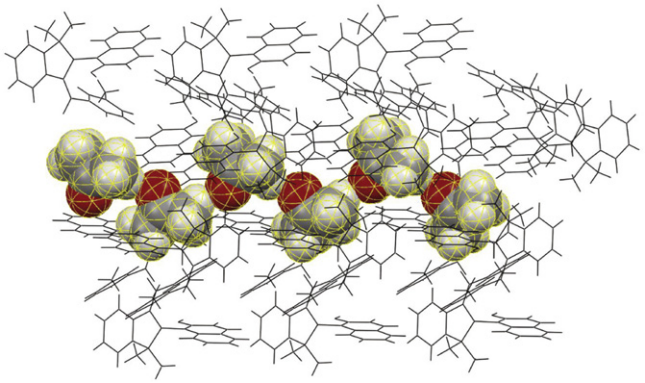

Fig. 9. PM6-Calculated partial structure extracted from **5d**·acetone complex.

From the PM6 method, the CH/O interaction between the methyl hydrogen and carbonyl oxygen of acetone was predicted. The average distances between C–H···O and C(H)···O are 2.246 and 3.283 Å, respectively. The interaction between the host and guest molecules is considered to be mainly the result of *van der* Waals forces. The calculated guest plane is somewhat rotated around the *c*-axis compared to that in the crystal structure (see Figs. S6 and S8). This suggests that the host–guest CH/π interaction expected from X-ray analysis is not strong enough to hold acetone in a uniform restricted space.

The phenolic OH group of the host is expected to stabilize the host–host network by hydrogen bonds. In the packing structure of the **5d**·acetone complex, the two host molecules form a dimeric unit by means of intermolecular hydrogen bonding and along the host channel, the guests (acetone) are infinitely linked to other neighboring guests by weak CH/O interactions *via* the carbonyl oxygen. The dimer was linked with the neighboring host by a weak CH/N interaction. The fact that the guest-free crystal of **5d** was obtained from slow evaporation of protic solvent (i.e., ethanol)[16] suggests that the OH/O and CH/N interaction are necessary for the construction of the host–host network in the formation of the inclusion cavity.

It is interesting that even if the guest is a strong hydrogen-bond acceptor, such as acetone, the host, which contains the ArOH group, does not form hydrogen bonds with the guest. This information may be useful for the design of new hydroxylic clathrate hosts containing aromatic rings. Reinvestigation of other atropisomers (**5**) as new clathrate hosts is in progress.

In summary, the inclusion properties of the clathrate crystals of **4a** and **4b** have been investigated by means of X-ray crystallography. Benzene is embedded in a host lattice constituted of the intermolecular 'edge-to-face' interactions of the host aromatic rings.

Inter- and intra-molecular edge-to-face attractive interactions become important factors in stabilization of ground-state and transition-state geometries and determination of reaction selectivity. PM6 semi-empirical MO calculations seem to provide an excellent clue for prediction of aromatic CH/π interaction. The present work serves as a calculation model for understanding molecular recognition in organic reactions.

4. Experimental section

4.1. Materials

(4-Substitutedphenyl)(2-hydroxy-3,3-dimethylindolin-1-yl) methanones (**4a**–**d**) were prepared by the addition of substituted benzoyl chloride to 3,3-dimethyl-3*H*-indole (**1**) followed by treatment of the corresponding 2-chloro derivatives (**3**) with water.[4b] Compound **5d** (*anti*) was prepared according to the previously reported method.[4c]

4.2. Thermal analysis

Thermal analyses of **4a**, **4b**, and **5d**·acetone were performed on a Shimadzu DTG-50/50H simultaneous TG/DTA instrument.

4.3. Crystal structure analysis

The single crystals for the 2:1 inclusion complexes of **4a** and **4b** with benzene were prepared by slow evaporation of its benzene solution at room temperature. All measurements were performed on a Rigaku RAXIS RAPID imaging plate area detector with graphite-monochromated Mo Kα radiation (λ=0.7107 Å). The data were collected at a temperature of 23±1 °C to a maximum 2θ value of 55°. The structure was solved by direct method (SIR2008[17a]), and all hydrogen atoms were located at calculated positions. The structure was refined by a full-matrix least-squares technique using anisotropic thermal parameters for non-hydrogen atoms and a riding model for hydrogen atoms. All calculations were performed using the crystallographic software package Crystal Structure.[17b,c] These X-ray crystallographic data have been deposited at the Cambridge Crystallographic Data Centre (CCDC).

*4.3.1. Crystal data of **4a**·benzene.* $C_{20}H_{19}N_2O_4$, M=351.38, triclinic, space group $P(-1)$ (#2), a=8.5800 (12), b=15.4573 (15), c=7.1887 (8) Å, α=102.557 (5)°, β=97.441 (4)°, γ=101.661 (4)°, V=896.2 (2) Å^3, Z=2, Dc=1.302 g/cm^3, R=0.080, R_w=0.170, GOF=1.000, CCDC ref. No. 825568; **4b**·benzene $C_{20}H_{19}ClNO_2$, M=340.83, monoclinic, space group $P2_1/n$ (#14), a=10.3816 (6), b=12.5590 (9), c=14.6984 (8) Å, β=108.7417 (13)°, V=1814.8 (2) Å^3, Z=4, Dc=1.247 g/cm^3, R=0.083, R_w=0.160, GOF=1.001, CCDC ref. No. 825569; **4c** $C_{17}H_{16}N_2O_4$, M=312.32, monoclinic, space group $P2_1/c$ (#14), a=9.6035 (12), b=110.3597 (9), c=15.5415 (13) Å, β=97.953 (4)°, V=1531.3 (3) Å^3, Z=4, Dc=1.355 g/cm^3, R=0.068, R_w=0.122, GOF=1.002, CCDC ref. No. 825570.

The packing structures of these complexes are shown in the provided Supplementary data (Figs. S4–S6).

4.4. Molecular orbital (MO) calculations

Semi-empirical MO (PM6, PM3, AM1) calculations were run through Winmostar[18] interface using MOPAC2009[9] on a DELL Dimension9200 computer.

Supplementary data

Supplementary data associated with this article can be found, in the online version, at doi:10.1016/j.tet.2011.07.021.

References and notes

1. (a) Nishio, M.; Hirota, M.; Umezawa, Y. *The CH/π Interaction; Evidence Nature and Consequences*; Wiley: New York, NY, 1998; (b) Takahashi, O.; Kohno, Y.; Nishio, M. *Chem. Rev.* **2010**, *110*, 6049–6076; (c) Recent lists of articles relating CH/π interaction are available from http://www.tim.hi-ho.ne.jp/dionisio/page/other.html.

2. Suezawa, H.; Yoshida, T.; Hirota, M.; Takahashi, H.; Umezawa, Y.; Honda, K.; Tsuboyama, S.; Nishio, M. *J. Chem. Soc., Perkin Trans. 2* **2001**, 2053–2058.
3. (a) Umezawa, Y.; Nishio, M. *Bioorg. Med. Chem.* **1998**, *6*, 493–504; (b) Umezawa, Y.; Nishio, M. *Bioorg. Med. Chem.* **2000**, *8*, 2643–2650; (c) Umezawa, Y.; Nishio, M. *Nucleic Acids Res.* **2002**, *30*, 2183–2192; (d) Umezawa, Y.; Nishio, M. *Biopolymers* **2005**, *79*, 248–258.
4. (a) Harano, K.; Yasuda, M.; Ida, Y.; Komori, T.; Taguchi, T. *Cryst. Struct. Commun.* **1981**, *10*, 165–171; (b) Eto, M.; Harano, K.; Hisano, T.; Kitamura, T. *J. Heterocycl. Chem.* **1992**, *29*, 311–315; (c) Kitamura, T.; Harano, K.; Hisano, T. *Chem. Pharm. Bull.* **1992**, *40*, 2255–2261; (d) Eto, M.; Ito, F.; Kitamura, T.; Harano, K. *Heterocycles* **1994**, *38*, 2159–2163; (e) Eto, M.; Ito, F.; Kitamura, T.; Harano, K. *Heterocycles* **1996**, *43*, 1159–1163; (f) Watanabe, A.; Moriguchi, M.; Ito, F.; Yoshitake, Y.; Eto, M.; Harano, K. *Heterocycles* **2000**, *53*, 1–6; (g) Ito, F.; Moriguchi, T.; Yoshitake, Y.; Eto, M.; Yahara, S.; Harano, K. *Chem. Pharm. Bull.* **2003**, *51*, 688–696; (h) Watanabe, A.; Yamaguchi, K.; Ito, F.; Yoshitake, Y.; Harano, K. *Heterocycles* **2007**, *71*, 343–359; (i) Eto, M.; Ito, F.; Sato, H.; Shinohara, I.; Yamaguchi, K.; Yoshitake, Y.; Harano, K. *Heterocycles* **2009**, *78*, 1485–1496; (j) Eto, M.; Yamaguchi, K.; Shinohara, I.; Ito, F.; Yoshitake, Y.; Harano, K. *Tetrahedron* **2010**, *66*, 898–903.
5. Johnson, C. K. *ORTEP-II: A FORTRAN Thermal-Ellipsoid Plot Program for Crystal Structure Illustrations*; National Laboratory: Oak Ridge, 1976; Report ORNL-5138.
6. (a) Taylor, R.; Kennard, O. *J. Am. Chem. Soc.* **1982**, *104*, 5063–5070; (b) Desiraju, G. R. *Acc. Chem. Res.* **1991**, *24*, 290–296; (c) Steiner, T.; Kanters, J. A.; Kroon, J. A. *Chem. Commun.* **1996**, 1277–1278; (d) Steiner, T. *Cryst. Rev.* **1996**, *6*, 1–57.
7. Dewar, M. J. S.; Zoebisch, E. G.; Healy, E. F.; Stewart, J. J. P. *J. Am. Chem. Soc.* **1985**, *107*, 3902–3909.
8. Stewart, J. J. P. *J. Comput. Chem.* **1989**, *10*, 209–220.
9. MOPAC2009: Stewart, J.J.P. *Stewart Computational Chemistry, Version 9.062M* (http://OpenMOPAC.net).
10. To confirm the reliability of PM6 method, typical compounds (**A**,[19] **B**,[20] **C**[21]) containing intramolecular edge-to-face conformation were examined.

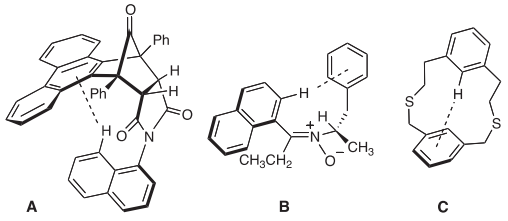

The calculations well reproduced the structural features of the crystal geometry. For details of the PM6 investigations see the Supplementary data (Figs. S9–S11).

11. In the calculation, the central benzene molecule is freely optimized and the coordinates of surrounding molecules are frozen. The stabilization energy due to inclusion of benzene by four edge-to-face interactions is calculated.
12. Frisch, M. J.; Trucks, G. W.; Schlegel, H. B.; Scuseria, G. E.; Robb, M. A.; Cheeseman, J. R.; Montgomery, J. A., Jr.; Vreven, T.; Kudin, K. N.; Burant, J. C.; Millam, J. M.; Iyengar, S. S.; Tomasi, J.; Barone, V.; Mennucci, B.; Cossi, M.; Scalmani, G.; Rega, N.; Petersson, G. A.; Nakatsuji, H.; Hada, M.; Ehara, M.; Toyota, K.; Fukuda, R.; Hasegawa, J.; Ishida, M.; Nakajima, T.; Honda, Y.; Kitao, O.; Nakai, H.; Klene, M.; Li, X.; Knox, J. E.; Hratchian, H. P.; Cross, J. B.; Bakken, V.; Adamo, C.; Jaramillo, J.; Gomperts, R.; Stratmann, R. E.; Yazyev, O.; Austin, A. J.; Cammi, R.; Pomelli, C.; Ochterski, J. W.; Ayala, P. Y.; Morokuma, K.; Voth, G. A.; Salvador, P.; Dannenberg, J. J.; Zakrzewski, V. G.; Dapprich, S.; Daniels, A. D.; Strain, M. C.; Farkas, O.; Malick, D. K.; Rabuck, A. D.; Raghavachari, K.; Foresman, J. B.; Ortiz, J. V.; Cui, Q.; Baboul, A. G.; Clifford, S.; Cioslowski, J.; Stefanov, B. B.; Liu, G.; Liashenko, A.; Piskorz, P.; Komaromi, I.; Martin, R. L.; Fox, D. J.; Keith, T.; Al-Laham, M. A.; Peng, C. Y.; Nanayakkara, A.; Challacombe, M.; Gill, P. M. W.; Johnson, B.; Chen, W.; Wong, M. W.; Gonzalez, C.; Pople, J. A. *Gaussian 03, Revision C.02*; Gaussian,: Wallingford CT, 2004.
13. The DTA (differential thermal analysis) of **5d**·acetone complex showed a broad endothermic peak corresponding to the guest losses at 89 °C, followed by an endothermic peak at 221 °C caused by melting of the host. The total weight loss was 7.7%. The value is much smaller than the expected loss of 15.2% for a 1:1 ratio. These facts indicated that the measurement sample used is the mixture of the complex and the guest-free crystal (see Fig. S3).
14. A reviewer pointed out that the existence of the CH/N interaction between the methyl hydrogen and NCO π system is a questionable. Only a few examples (NH/N type) of protonation toward amide nitrogen atom were known as 'amide proton sponge'. (a) Cox, C.; Wack, H.; Lectka, T. *Angew. Chem., Int. Ed.* **1999**, *38*, 798–800; (b) Cox, C.; Lectka, T. *Org. Lett.* **1999**, *1*, 749–752.
15. B3LYP/6-31G(d) estimated ground-state structures and energies of **5** (*anti*) with/without intramolecular OH/N interaction are depicted as follows: the GS_a including intramolecular OH/N hydrogen bond between the OH and NCO moiety is *ca.* 2.3 kcal/mol more stable than that of GS_bThe details will be reported in the near future.

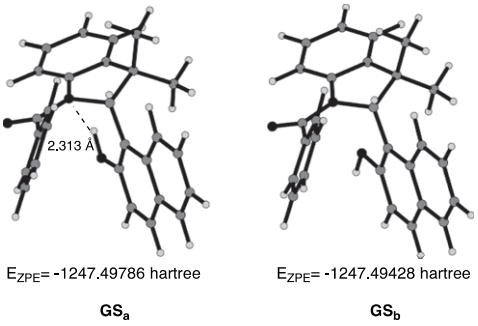

16. Recrystallization of **5d** from ethanol afforded colorless prisms. The elemental analysis indicates that the crystal did not enclathrate ethanol. Calcd for $C_{28}H_{27}NO_2$: C, 82.53: H, 6.18: N, 3.44. Found: C, 82.36, H, 6.21: N, 3.64. The X-ray analysis also indicated the crystal is guest-free. The crystal data of guest-free **5d** are as follows: $C_{28}H_{25}NO_2$, M=407.5, triclinic, space group $P(-1)$ (#2), a=12.4728 (16), b=13.676 (3), c=14.200 (2) Å, α=88.318 (5)°, β=67.844 (4)°, γ=84.314 (5)°, V=2232.3 (6) Å^3, Z=4, Dc=1.212 g/cm^3, R=0.089, R_w=0.112, GOF=1.063. The maximum peaks on the final difference Fourier map corresponded to 0.64 e/Å^3.
17. (a) SIR2008: Burla, M. C.; Caliandro, R.; Camalli, M.; Carrozzini, B.; Cascarano, G.; De Caro, L.; Giacovazzo, C.; Polidori, G.; Siliqi, D.; Spagna, R. *J. Appl. Crystallogr.* **2007**, *40*, 609–613; (b) *CrystalStructure 4.0: Crystal Structure Analysis Package*; Rigaku Corporation: Tokyo 196-8666, Japan, 2000–2010; (c) CRYSTALS Issue 11: Carruthers, J. R.; Rollett, J. S.; Betteridge, P. W.; Kinna, D.; Pearce, L.; Larsen, A.; Gabe, E.; Chemical Crystallography Laboratory: Oxford, UK, 1999.
18. Senda, N. *Idemitsu Technical Report* **2006**, *49*, 106–111.
19. Yoshitake, Y.; Misaka, J.; Setoguchi, K.; Abe, M.; Kawaji, T.; Eto, M.; Harano, K. *J. Chem. Soc., Perkin Trans. 2* **2002**, *9*, 1161–1169.
20. Boyd, D. R.; Evans, T. A.; Jennings, W. B.; Malone, J. F.; O'Sullivan, W.; Smith, A. *Chem. Commun.* **1996**, 2269–2270.
21. Schladetzky, K. D.; Haque, T. S.; Gellman, S. H. *J. Org. Chem.* **1995**, *60*, 4108–4113.